A well-balanced Discontinuous-Galerkin Lagrange-Projection scheme for the Shallow Water Equations

Christophe Chalons, Maxime Stauffert

A well-balanced Discontinuous-Galerkin Lagrange-Projection scheme for the Shallow Water Equations

Christophe Chalons* Maxime Stauffert†

October 9, 2017

Abstract. This work considers the Shallow Water equations (SWE) and proposes a high order conservative scheme based on a Lagrange-Projection decomposition. The high order in space and time are achieved using Discontinuous-Galerkin (DG) and Runge-Kutta (RK) strategies. The use of a Lagrange-Projection decomposition enables the use of time steps that are not constrained by the sound speed thanks to an implicit treatment of the acoustic waves (Lagrange step), while the transport waves (Projection step) are treated explicitly. We prove that our scheme satisfies the well-balanced property as well as non linear stability properties. Numerical evidences are also given.

Keywords. Shallow Water Equations, high order discontinuous Galerkin schemes, Lagrange-Projection decomposition, implicit explicit, large time steps, well-balanced property

1 Introduction

We are interested in the shallow water equations

$$\begin{cases} \partial_t h + \partial_x(hu) = 0, \\ \partial_t(hu) + \partial_x\left(hu^2 + p\right) = -gh\partial_x z, \end{cases} \tag{1}$$

where $h > 0$ is the water height, u the velocity, z the topography height and $p = gh^2/2$ is the pressure term where $g > 0$ is the gravity constant. The unknowns depend on the space and time variables x and t, with $x \in \mathbb{R}$ and $t \in [0, \infty)$. At time $t = 0$, the model is supplemented with a given initial data $h(x, t = 0) = h_0(x)$ and $u(x, t = 0) = u_0(x)$. The entropy inequality associated with (1) can be written either in a non conservative form as follows,

$$\partial_t hE\left(w\right) + \partial_x \mathcal{F}\left(w\right) \leqslant -ghu\partial_x z \tag{2}$$

where $w = (h, hu)^T$ and, setting $e(h) = gh/2$,

$$hE\left(w\right) = h\frac{u^2}{2} + he(h), \quad \mathcal{F}\left(w\right) = \left(\frac{u^2}{2} + gh\right)hu, \tag{3}$$

or in conservative form as follows,

$$\partial_t h\tilde{E}\left(w\,, z\right) + \partial_x \tilde{\mathcal{F}}\left(w\,, z\right) \leqslant 0\,, \tag{4}$$

*Laboratoire de Mathématiques de Versailles, UVSQ, CNRS, Université Paris-Saclay, 78035 Versailles, France, (christophe.chalons@uvsq.fr).

†Laboratoire de Mathématiques de Versailles, UVSQ, CNRS, Université Paris-Saclay, 78035 Versailles, France, (maxime.stauffert@uvsq.fr).

with the *conservative entropy* $\tilde{E}$ and the associated flux $\tilde{\mathcal{F}}$ defined by,

$$h\tilde{E}(w,z) = hE(w) + ghz \quad \text{and} \quad \tilde{\mathcal{F}}(w,z) = \mathcal{F}(w) + ghuz\,. \tag{5}$$

Note that the proposed numerical scheme will satisfy a discrete form of the non conservative entropy inequality (2).

The aim of this paper is to propose a high order discretization of (1) based on a Lagrange-Projection decomposition and using Discontinuous-Galerkin (DG) [9, 16] and Runge-Kutta (RK) [14] strategies for the space and time variables respectively. We will also pay a particular attention to the well-known well-balanced property, see for instance [2, 11], the references therein and the large litterature on this topic.

The proposed strategy can be understood as a natural extension to the present setting of the first-order well-balanced Lagrange-Projection scheme developed in [7] for the shallow water equations, and of the high order Lagrange-Projection scheme introduced in [8] (see also [13] for a similar approach) for the barotropic gas dynamics equations. The Lagrange-Projection (or equivalently Lagrange-Remap) decomposition naturally decouples the acoustic and transport terms of (1). It proved to be useful and very efficient when considering subsonic or low-Mach number flows. In this case, the CFL restriction of Godunov-type schemes is driven by the acoustic waves and can be very restrictive. As we will see, the Lagrange-Projection strategy allows for a very natural implicit-explicit scheme with a CFL restriction based on the (slow) transport waves and not on the (fast) acoustic waves, see the pionneering paper [10]. Note that the low-Mach (or low-Froud in the present setting of shallow water equations) limit using the same techniques as in [4, 5, 6] will not be considered in the present paper but is the topic of current research. Here, we focus on the design of a high order well-balanced implicit explicit scheme in a Lagrange-Projection framework.

The outline of the paper is as follows. We firt briefly recall the Lagrange-Projection decomposition and the underlying first-order finite volume scheme in the next section. We then formulate this scheme using a Discontinous-Galerkin framework in Section 3. The stability and well-balanced properties are collected in Section 4. At last, Section 5 illustrates the behaviours of our schemes on several test cases.

2 Lagrange-Projection decomposition and first-order relaxation scheme

In this section, we briefly present the Lagrange-Projection decomposition considered in this paper as well as the corresponding first-order finite volume scheme based on a relaxation approach. Note from now on that the latter will provide a natural linearization of the pressure term p, which will be helpful in order to define an efficient implicit discretization of the Lagrangian step.

Operator splitting decomposition and relaxation approximation. Using the chain rule for the space derivatives of (1), the Lagrange-Projection decomposition consists in first solving

$$\begin{cases} \partial_t h + h\partial_x u = 0, \\ \partial_t(hu) + hu\partial_x u + \partial_x p = -gh\partial_x z, \end{cases} \tag{6}$$

which gives in Lagrangian coordinates $\tau\partial_x = \partial_m$, with $\tau = 1/h$,

$$\begin{cases} \partial_t \tau - \partial_m u = 0, \\ \partial_t u + \partial_m p = -\dfrac{g}{\tau}\partial_m z, \end{cases} \tag{7}$$

and then the transport system

$$\begin{cases} \partial_t h + u\partial_x h = 0, \\ \partial_t(hu) + u\partial_x(hu) = 0. \end{cases} \tag{8}$$

It is interesting to note that the strictly hyperbolic system (7) with eigenvalues $\pm hc$ where the sound speed c equals $\sqrt{p'(h)}$ accounts for the acoustic waves of (1) (or equivalently (6)). On the other hand, the hyperbolic system (8) with eigenvalues u accounts for the transport waves of (1).

In the following, the Lagrangian system (7) will be treated considering the following relaxation approximation [12], [15], [2]

$$\begin{cases} \partial_t \tau - \partial_m u = 0, \\ \partial_t u + \partial_m \Pi = -\dfrac{g}{\tau}\partial_m z, \\ \partial_t \Pi + a^2 \partial_m u = \lambda \left(p - \Pi\right). \end{cases} \tag{9}$$

Here, the new variable Π represents a linearization of the real pressure p, the constant parameter a is a linearization of the Lagrangian sound speed hc such that the sub-characteristic condition $a > hc$ is satisfied, and the relaxation parameter λ allows to recover $\Pi = p$ and the original system (7) in the asymptotic regime $\lambda \to \infty$. As usual, the relaxation system will be solved using a splitting strategy which consists in first setting $\Pi = p$ at initial time (which is formally equivalent to considering $\lambda \to \infty$), and then solving the relaxation system (9) with $\lambda = 0$.

First-order well-balanced Lagrange-Projection scheme. In this paragraph, we briefly recall the first-order finite volume scheme given in [7] and associated with the above Lagrange-Projection decomposition and relaxation approximation. Space and time will be discretized using constant space step Δx and time step Δt. We will consider a set of cells $\kappa_j = [x_{j-1/2}, x_{j+1/2})$ and instants $t^n = n\Delta t$, where $x_{j+1/2} = j\Delta x$ and $x_j = (x_{j-1/2} + x_{j+1/2})/2$ are respectively the cell interfaces and cell centers, for $j \in \mathbb{Z}$ and $n \in \mathbb{N}$.

Following [7] and using standard notations, the Lagrangian step is discretized by

$$\begin{cases} \tau_j^{n+1-} = L_j^n \tau_j^n, \\ L_j^n (hu)_j^{n+1-} = (hu)_j^n - \dfrac{\Delta t}{\Delta x}(\Pi_{j+1/2}^{*,\alpha} - \Pi_{j-1/2}^{*,\alpha}) - \Delta t \left\{gh\partial_x z\right\}_j^n, \\ L_j^n (h\Pi)_j^{n+1-} = (h\Pi)_j^n + a^2 \dfrac{\Delta t}{\Delta x}(u_{j+1/2}^{*,\alpha} - u_{j-1/2}^{*,\alpha}), \end{cases}$$

with

$$L_j^{n,\alpha} = 1 + \frac{\Delta t}{\Delta x}(u_{j+1/2}^{*,\alpha} - u_{j-1/2}^{*,\alpha}),$$

$$u_{j+1/2}^{*,\alpha} = \frac{1}{2}(u_j^\alpha + u_{j+1}^\alpha) - \frac{1}{2a}(\Pi_{j+1}^\alpha - \Pi_j^\alpha) - \frac{\Delta x}{2a}\{gh\partial_x z\}_{j+1/2},$$

$$\Pi_{j+1/2}^{*,\alpha} = \frac{1}{2}(\Pi_j^\alpha + \Pi_{j+1}^\alpha) - \frac{a}{2}(u_{j+1}^\alpha - u_j^\alpha),$$

and

$$\{gh\partial_x z\}_j^n = \frac{1}{2}(\{gh\partial_x z\}_{j-1/2}^n + \{gh\partial_x z\}_{j+1/2}^n),$$

$$\{gh\partial_x z\}_{j+1/2}^n = g\frac{h_j^n + h_{j+1}^n}{2}\frac{z_{j+1} - z_j}{\Delta x}.$$

In the above formulas, $\Pi_j^n = p_j^n = p(h_j^n)$ for all j and α refers to the time index and equals n (respectively $n+1-$) if the scheme is taken to be explicit (resp. implicit) in time. Note that the source term is always taken at time t^n, even for the time implicit scheme. In the following, we will be especially interested in the choice $\alpha = n+1-$ in order to get rid of the usual acoustic CFL restriction.

As far as the transport step is concerned, a natural discretization of (8) reads

$$\begin{cases} h_j^{n+1} = h_j^{n+1-} - \dfrac{\Delta t}{\Delta x}\left[\left(u_{j+1/2}^{*,\alpha}\right)_- \left(h_{j+1}^{n+1-} - h_j^{n+1-}\right) + \left(u_{j-1/2}^{*,\alpha}\right)_+ \left(h_j^{n+1-} - h_{j-1}^{n+1-}\right)\right], \\ (hu)_j^{n+1} = (hu)_j^{n+1-} - \dfrac{\Delta t}{\Delta x}\left[\left(u_{j+1/2}^{*,\alpha}\right)_- \left((hu)_{j+1}^{n+1-} - (hu)_j^{n+1-}\right) + \left(u_{j-1/2}^{*,\alpha}\right)_+ \left((hu)_j^{n+1-} - (hu)_{j-1}^{n+1-}\right)\right], \end{cases} \tag{10}$$

where $\left(u^{*,\alpha}_{j\pm1/2}\right)_+ = \max(u^{*,\alpha}_{j\pm1/2},0)$ and $\left(u^{*,\alpha}_{j\pm1/2}\right)_- = \min(u^{*,\alpha}_{j\pm1/2},0)$ for all j.

At last, we underline that easy calculations give that the whole scheme is conservative in the usual sense of finite volume methods and writes

$$\begin{cases} h_j^{n+1} = h_j^n - \dfrac{\Delta t}{\Delta x}\big(h^{*,n+1-}_{j+1/2}u^{*,\alpha}_{j+1/2} - h^{*,n+1-}_{j-1/2}u^{*,\alpha}_{j-1/2}\big), \\ (hu)_j^{n+1} = (hu)_j^n - \dfrac{\Delta t}{\Delta x}\big((hu)^{*,n+1-}_{j+1/2}u^{*,\alpha}_{j+1/2} + \Pi^{*,\alpha}_{j+1/2} - (hu)^{*,n+1-}_{j-1/2}u^{*,\alpha}_{j-1/2} - \Pi^{*,\alpha}_{j-1/2}\big) - \Delta t\{gh\partial_x z\}_j^n, \end{cases} \tag{11}$$

with, for $X = h, hu$,

$$X^{*,n+1-}_{j+1/2} = \begin{cases} X_j^{n+1-}, & \text{if } u^{*,\alpha}_{j+1/2} \geq 0, \\ X_{j+1}^{n+1-}, & \text{if } u^{*,\alpha}_{j+1/2} \leq 0. \end{cases}$$

We refer the reader to [7] for more details and the non linear stability properties satisfied by this first order finite volume numerical scheme. Let us just underline that it satisfies the well-balanced property for the lake at rest. More precisely, if the discrete fluid state at time t^n matches the lake at rest conditions $u_j^n = 0$ and $h_j^n + z_j^n = h_{j+1}^n + z_{j+1}^n$ for all j, then $h_j^{n+1} = h_j^n$ and $u_j^{n+1} = u_j^n$.

The aim of the next section is to develop a high order and well-balanced extension of this scheme using Discontinuous-Galerkin and Runge-Kutta techniques for the space and time variables respectively.

3 Discontinuous-Galerkin discretization

We begin this section by introducing the notations of the DG discretization. Recall that the DG approach considers that the approximate solution at each time t^n is defined on each cell κ_j by a polynomial in space of order less or equal than p for a given integer $p \geq 1$ ($p = 0$ corresponds to the usual first-order and piecewise constant finite volume scheme). With this in mind, we consider the $(p+1)$ Lagrange polynomials $\{\ell_i\}_{i=0,\dots,p}$ associated with the Gauss-Lobatto quadrature points in $[-1,1]$. More precisely, denoting $-1 = s_0 < s_1 < \cdots < s_p = 1$ the $p+1$ Gauss-Lobatto quadrature points, ℓ_i is defined by the relations $\ell_i(s_k) = \delta_{i,k}$ for $k = 0,...,p$, where δ is the Kronecker symbol. Then, in each cell κ_j, we define the shifted Lagrange polynomials $\Phi_{i,j}$ by $\Phi_{i,j}(x) = \ell_i\big(\frac{2}{\Delta x}(x - x_j)\big)$ and we take $\{\Phi_{i,j}\}_{i=0,\dots,p}$ as a basis for polynomials or order less or equal than p on κ_j. Note that for all j

$$\sum_{i=0}^{p} \Phi_{i,j}(x) = 1. \tag{12}$$

If we denote by $X_{\Delta x}$ the DG approximation of X, we thus have $X_{\Delta x}(x,t) = \sum_{k=0}^p X_{k,j}(t)\,\Phi_{k,j}(x)$ for all $x \in \kappa_j$, where the coefficients $X_{k,j}$ depend on the time t and correspond to the value of X at the shifted Gauss-Lobatto quadrature points $x_{k,j} = x_j + \frac{\Delta x}{2}s_k$.

Before entering the details of the numerical approximation, let us briefly recall that the Gauss-Lobatto quadrature formula for evaluating the space integral of a given function $f : \kappa_j \times \mathbb{R}^+ \to \mathbb{R}$ writes

$$\int_{\kappa_j} f(x,t)\,\mathrm{d}x \approx \frac{\Delta x}{2}\sum_{k=0}^{p} \omega_k f(x_{k,j},t), \tag{13}$$

where ω_k are the weights of the Gauss-Lobatto quadrature. It is well-known that this formula is exact as soon as f is a polynomial of order less or equal than $(2p-1)$ with respect to x on κ_j. In particular, we have

$$\sum_{k=0}^{p} \frac{\omega_k}{2} = 1. \tag{14}$$

Note also that the integral $\int_{\kappa_j} \Phi_{i,j}(x)\Phi_{k,j}(x)\,\mathrm{d}x$ will be therefore approximated by $\frac{\Delta x}{2}\omega_i\delta_{i,k}$ in the following. At last, note that the piecewise constant case $p=0$ can be also considered in this framework provided that we set $s_0=0$, $\Phi_{0,j}=1$ and $\omega_0=2$.

3.1 The acoustic step

We begin with the acoustic step (9) with $\lambda=0$.

Time discretization ($t^n \to t^{n+1}$). Multiplying the three equations by $\Phi_{i,j}$, integrating over κ_j, and considering the piecewise polynomial approximations $X_{\Delta x}$ for $X=\tau,u,\Pi$ easily leads to

$$\begin{cases} \dfrac{\Delta x}{2}\omega_i\partial_t\tau_{i,j}(t) - \displaystyle\int_{\kappa_j}\Phi_{i,j}(x)\partial_m u(x,t)\,\mathrm{d}x = 0, \\ \dfrac{\Delta x}{2}\omega_i\partial_t u_{i,j}(t) + \displaystyle\int_{\kappa_j}\Phi_{i,j}(x)\partial_m \Pi(x,t)\,\mathrm{d}x = -\int_{\kappa_j}\Phi_{i,j}(x)\frac{g}{\tau(x,t)}\partial_m z(x)\,\mathrm{d}x, \\ \dfrac{\Delta x}{2}\omega_i\partial_t \Pi_{i,j}(t) + a^2\displaystyle\int_{\kappa_j}\Phi_{i,j}(x)\partial_m u(x,t)\,\mathrm{d}x = 0, \end{cases}$$

that we discretize in time by

$$\begin{cases} \tau_{i,j}^{n+1-} = \tau_{i,j}^n + \dfrac{2\Delta t}{\omega_i\Delta x}\displaystyle\int_{\kappa_j}\Phi_{i,j}(x)\partial_m u(x,t^\alpha)\,\mathrm{d}x, \\ u_{i,j}^{n+1-} = u_{i,j}^n - \dfrac{2\Delta t}{\omega_i\Delta x}\displaystyle\int_{\kappa_j}\Phi_{i,j}(x)\partial_m \Pi(x,t^\alpha)\,\mathrm{d}x - \dfrac{2\Delta t}{\omega_i\Delta x}\displaystyle\int_{\kappa_j}\Phi_{i,j}(x)\frac{g}{\tau(x,t^n)}\partial_m z(x)\,\mathrm{d}x, \\ \Pi_{i,j}^{n+1-} = \Pi_{i,j}^n - a^2\dfrac{2\Delta t}{\omega_i\Delta x}\displaystyle\int_{\kappa_j}\Phi_{i,j}(x)\partial_m u(x,t^\alpha)\,\mathrm{d}x, \end{cases} \tag{15}$$

where $\alpha=n$ or $\alpha=n+1-$ depending on whether the time discretization is taken to be explicit or implicit. Again, we are especially interested in this work in the case $\alpha=n+1-$.

Volume integrals and flux calculations. We first aim at approximating the integrals $\int_{\kappa_j}\Phi_{i,j}(x)\partial_m X(x,t^\alpha)\,\mathrm{d}x$ with $X=u,\Pi$. Observe that

$$\int_{\kappa_j}\Phi_{i,j}(x)\partial_m X(x,t^\alpha)\,\mathrm{d}x \approx \frac{\Delta x}{2}\omega_i\tau_{i,j}^n\partial_x X(x_{i,j},t^\alpha)\,\mathrm{d}x = \tau_{i,j}^n\int_{\kappa_j}\Phi_{i,j}(x)\partial_x X(x,t^\alpha)\,\mathrm{d}x,$$

the last equality is indeed exact since X and Φ are polynomials of order less or equal than p, so that $\Phi_{i,j}\partial_x X(\cdot,t)$ is of order less or equal than $(2p-1)$. The objective is now to use one integration by part to move the derivative from X to Φ, and to use the numerical fluxes to evaluate the interfacial terms, which gives

$$\int_{\kappa_j}\Phi_{i,j}(x)\partial_x X(x,t^\alpha)\,\mathrm{d}x = \delta_{i,p}X_{j+1/2}^{*,\alpha} - \delta_{i,0}X_{j-1/2}^{*,\alpha} - \frac{\Delta x}{2}\sum_{k=0}^{p}\omega_k X_{k,j}^\alpha\partial_x\Phi_{i,j}(x_{k,j}).$$

Note that in the above formula and the following ones, the star quantities $X_{j+1/2}^{*,\alpha}$ with $X=u,\Pi$ will be defined using a similar definition as in Section 2, namely

$$u_{j+1/2}^{*,\alpha} = \frac{1}{2}(u_{p,j}^\alpha + u_{0,j+1}^\alpha) - \frac{1}{2a}(\Pi_{0,j+1}^\alpha - \Pi_{p,j}^\alpha) - \frac{\Delta x}{2a}\{gh\partial_x z\}_{j+1/2}, \tag{16}$$

$$\Pi_{j+1/2}^{*,\alpha} = \frac{1}{2}(\Pi_{p,j}^\alpha + \Pi_{0,j+1}^\alpha) - \frac{a}{2}(u_{0,j+1}^\alpha - u_{p,j}^\alpha), \tag{17}$$

with

$$\{gh\partial_x z\}^n_{j+1/2} = g\frac{h^n_{p,j} + h^n_{0,j+1}}{2}\frac{z_{0,j+1} - z_{p,j}}{\Delta x}. \tag{18}$$

In particular, our DG scheme will naturally degenerate towards the first-order scheme when $p = 0$. As far as the source term integral is concerned, it is not possible to move the derivative from z to Φ only. Therefore and according to (13), we simply write

$$\int_{\kappa_j} \Phi_{i,j}(x)\frac{g}{\tau(x,t^n)}\partial_m z(x)\,\mathrm{d}x \approx \tau^n_{i,j}\frac{\Delta x}{2}\left(\delta_{i,p}\{gh\partial_x z\}^n_{j+1/2} + \delta_{i,0}\{gh\partial_x z\}^n_{j-1/2} + \omega_i\{gh\partial_x z\}^n_{i,j}\right),$$

where

$$\{gh\partial_x z\}^n_{i,j} = gh^n_{i,j}\partial_x z(x_{i,j}). \tag{19}$$

Finally, we obtain from (15) and for the acoustic step the following update formulas

$$\begin{cases} \tau^{n+1-}_{i,j} = \tau^n_{i,j} + \dfrac{2\Delta t}{\omega_i\Delta x}\tau^n_{i,j}\left[\delta_{i,p}u^{*,\alpha}_{j+1/2} - \delta_{i,0}u^{*,\alpha}_{j-1/2} - \dfrac{\Delta x}{2}\displaystyle\sum_{k=0}^{p}\omega_k u^\alpha_{k,j}\partial_x\Phi_{i,j}(x_{k,j})\right] \\ \qquad\qquad = L^\alpha_{i,j}\tau^n_{i,j}, \\ L^\alpha_{i,j}(hu)^{n+1-}_{i,j} = (hu)^n_{i,j} - \dfrac{2\Delta t}{\omega_i\Delta x}\left[\delta_{i,p}\Pi^{*,\alpha}_{j+1/2} - \delta_{i,0}\Pi^{*,\alpha}_{j-1/2} - \dfrac{\Delta x}{2}\displaystyle\sum_{k=0}^{p}\omega_k\Pi^\alpha_{k,j}\partial_x\Phi_{i,j}(x_{k,j})\right] \\ \qquad\qquad - \Delta t\left[\dfrac{\delta_{i,p}}{\omega_p}\{gh\partial_x z\}_{j+1/2} + \dfrac{\delta_{i,0}}{\omega_0}\{gh\partial_x z\}_{j-1/2} + \{gh\partial_x z\}^n_{i,j}\right], \\ L^\alpha_{i,j}(h\Pi)^{n+1-}_{i,j} = (h\Pi)^n_{i,j} - a^2\dfrac{2\Delta t}{\omega_i\Delta x}\left[\delta_{i,p}u^{*,\alpha}_{j+1/2} - \delta_{i,0}u^{*,\alpha}_{j-1/2} - \dfrac{\Delta x}{2}\displaystyle\sum_{k=0}^{p}\omega_k u^\alpha_{k,j}\partial_x\Phi_{i,j}(x_{k,j})\right], \end{cases} \tag{20}$$

with

$$L^\alpha_{i,j} = 1 + \frac{2\Delta t}{\omega_i\Delta x}\left[\delta_{i,p}u^{*,\alpha}_{j+1/2} - \delta_{i,0}u^{*,\alpha}_{j-1/2} - \frac{\Delta x}{2}\sum_{k=0}^{p}\omega_k u^\alpha_{k,j}\partial_x\Phi_{i,j}(x_{k,j})\right]. \tag{21}$$

3.2 The transport step

We continue with the transport step (8).

Time discretization ($t^n \to t^{n+1}$). Along the lines of the acoustic step, we are led to set

$$\begin{cases} h^{n+1}_{i,j} = h^{n+1-}_{i,j} - \dfrac{2\Delta t}{\omega_i\Delta x}\displaystyle\int_{\kappa_j}\Phi_{i,j}(x)u(x,t^\alpha)\partial_x h(x,t^{n+1-})\,\mathrm{d}x, \\ (hu)^{n+1}_{i,j} = (hu)^{n+1-}_{i,j} - \dfrac{2\Delta t}{\omega_i\Delta x}\displaystyle\int_{\kappa_j}\Phi_{i,j}(x)u(x,t^\alpha)\partial_x(hu)(x,t^{n+1-})\,\mathrm{d}x. \end{cases} \tag{22}$$

Note that this transport step is always treated explicitly in time.

Volume integrals and flux calculations. We want to evaluate the integrals $\int_{\kappa_j}\Phi_{i,j}(x)u(x,t^\alpha)\partial_x X(x,t^{n+1-})\,\mathrm{d}x$ with $X = h, hu$. The same process as before leads to

$$\int_{\kappa_j}\Phi_{i,j}(x)u(x,t^\alpha)\partial_x X(x,t^{n+1-})\,\mathrm{d}x =$$

$$\delta_{i,p}X^{*,n+1-}_{j+1/2}u^{*,\alpha}_{j+1/2} - \delta_{i,0}X^{*,n+1-}_{j-1/2}u^{*,\alpha}_{j-1/2} - \int_{\kappa_j}(Xu)\partial_x\Phi_{i,j}\,\mathrm{d}x - X^{n+1-}_{i,j}\int_{\kappa_j}\Phi_{i,j}(x)\partial_x u(x,t^\alpha)\,\mathrm{d}x,$$

where we set

$$X^{*,\alpha}_{j+1/2} = \begin{cases} X^{\alpha}_{p,j}, & \text{if } u^{*,\alpha}_{j+1/2} \geq 0, \\ X^{\alpha}_{0,j+1}, & \text{if } u^{*,\alpha}_{j+1/2} \leq 0, \end{cases} \quad X = h, hu, \tag{23}$$

$$\int_{\kappa_j} \Phi_{i,j} \partial_x u(x,t^\alpha)\,\mathrm{d}x = \delta_{i,p} u^{*,\alpha}_{j+1/2} - \delta_{i,0} u^{*,\alpha}_{j-1/2} - \frac{\Delta x}{2} \sum_{k=0}^{p} \omega_k u^{\alpha}_{k,j} \partial_x \Phi_{i,j}(x_{k,j}),$$

and

$$\int_{\kappa_j} (Xu) \partial_x \Phi_{i,j}\,\mathrm{d}x = \frac{\Delta x}{2} \sum_{k=0}^{p} \omega_k X^{n+1-}_{k,j} u^{\alpha}_{k,j} \partial_x \Phi_{i,j}(x_{k,j}).$$

At last and from (22), we obtain for the transport step

$$\begin{cases} h^{n+1}_{i,j} = L^{\alpha}_{i,j} h^{n+1-}_{i,j} - \dfrac{2\Delta t}{\omega_i \Delta x} \left[\delta_{i,p} h^{*,n+1-}_{j+1/2} u^{*,\alpha}_{j+1/2} - \delta_{i,0} h^{*,n+1-}_{j-1/2} u^{*,\alpha}_{j-1/2} \right. \\ \qquad\qquad \left. - \dfrac{\Delta x}{2} \displaystyle\sum_{k=0}^{p} \omega_k h^{n+1-}_{k,j} u^{\alpha}_{k,j} \partial_x \Phi_{i,j}(x_{k,j}) \right], \\ (hu)^{n+1}_{i,j} = L^{\alpha}_{i,j} (hu)^{n+1-}_{i,j} - \dfrac{2\Delta t}{\omega_i \Delta x} \left[\delta_{i,p} (hu)^{*,n+1-}_{j+1/2} u^{*,\alpha}_{j+1/2} - \delta_{i,0} (hu)^{*,n+1-}_{j-1/2} u^{*,\alpha}_{j-1/2} \right. \\ \qquad\qquad \left. - \dfrac{\Delta x}{2} \displaystyle\sum_{k=0}^{p} \omega_k (hu)^{n+1-}_{k,j} u^{\alpha}_{k,j} \partial_x \Phi_{i,j}(x_{k,j}) \right]. \end{cases} \tag{24}$$

3.3 The whole scheme for the nodal and mean values

Gathering (20) and (24), it is easy to see that the whole Lagrange-Projection scheme writes

$$\begin{cases} h^{n+1}_{i,j} = h^{n}_{i,j} - \dfrac{2\Delta t}{\omega_i \Delta x} \left[\delta_{i,p} h^{*,n+1-}_{j+1/2} u^{*,\alpha}_{j+1/2} - \delta_{i,0} h^{*,n+1-}_{j-1/2} u^{*,\alpha}_{j-1/2} \right. \\ \qquad\qquad \left. - \dfrac{\Delta x}{2} \displaystyle\sum_{k=0}^{p} \omega_k h^{n+1-}_{k,j} u^{\alpha}_{k,j} \partial_x \Phi_{i,j}(x_{k,j}) \right], \\ (hu)^{n+1}_{i,j} = (hu)^{n}_{i,j} - \dfrac{2\Delta t}{\omega_i \Delta x} \left[\delta_{i,p} \Pi^{*,\alpha}_{j+1/2} - \delta_{i,0} \Pi^{*,\alpha}_{j-1/2} - \dfrac{\Delta x}{2} \displaystyle\sum_{k=0}^{p} \omega_k \Pi^{n+1-}_{k,j} \partial_x \Phi_{i,j}(x_{k,j}) \right] \\ \qquad\qquad - \dfrac{2\Delta t}{\omega_i \Delta x} \left[\delta_{i,p} (hu)^{*,n+1-}_{j+1/2} u^{*,\alpha}_{j+1/2} - \delta_{i,0} (hu)^{*,n+1-}_{j-1/2} u^{*,\alpha}_{j-1/2} \right. \\ \qquad\qquad \left. - \dfrac{\Delta x}{2} \displaystyle\sum_{k=0}^{p} \omega_k (hu)^{n+1-}_{k,j} u^{\alpha}_{k,j} \partial_x \Phi_{i,j}(x_{k,j}) \right] \\ \qquad\qquad - \Delta t \left[\dfrac{\delta_{i,p}}{\omega_p} \{gh\partial_x z\}_{j+1/2} + \dfrac{\delta_{i,0}}{\omega_0} \{gh\partial_x z\}_{j-1/2} + \{gh\partial_x z\}^{n}_{i,j} \right]. \end{cases} \tag{25}$$

In particular, the first-order scheme (11) is recovered when $p = 0$. On the other hand and in order to state the stability properties satisfied by this scheme, we will be interested in the evolution of the mean values $\overline{X}^{n+1}_j$ for $X = h, hu$, which are naturally defined for all n an j by

$$\overline{X}^{n+1}_j = \frac{1}{\Delta x} \int_{\kappa_j} X(x,t^n)\,\mathrm{d}x = \sum_{i=0}^{p} \frac{\omega_i}{2} X^{n}_{i,j}.$$

Multiplying (25) by $\omega_i/2$ and summing over i leads to (recall that (12) holds true so that $\sum_{i=0}^p \Phi'_{i,j}(x) = 0$)

$$\begin{cases} \overline{h}_j^{n+1} = \overline{h}_j^n - \dfrac{\Delta t}{\Delta x}\left[h_{j+1/2}^{*,n+1-} u_{j+1/2}^{*,\alpha} - h_{j-1/2}^{*,n+1-} u_{j-1/2}^{*,\alpha}\right], \\ \overline{(hu)}_j^{n+1} = \overline{(hu)}_j^n - \dfrac{\Delta t}{\Delta x}\left[\Pi_{j+1/2}^{*,\alpha} + (hu)_{j+1/2}^{*,n+1-} u_{j+1/2}^{*,\alpha} - \Pi_{j-1/2}^{*,\alpha} - (hu)_{j-1/2}^{*,n+1-} u_{j-1/2}^{*,\alpha}\right] \\ \qquad\qquad - \Delta t\left[\dfrac{\{gh\partial_x z\}_{j-1/2}^n + \{gh\partial_x z\}_{j+1/2}^n}{2} + \sum_{i=0}^p \dfrac{\omega_i}{2}\{gh\partial_x z\}_{i,j}^n\right]. \end{cases} \tag{26}$$

Note that by (13), the last term of (26) approximates a volume integral of the source term such that

$$\frac{1}{\Delta x}\int_{\kappa_j} gh\partial_x z \,\mathrm{d}x \approx \sum_{i=0}^p \frac{\omega_i}{2}\{gh\partial_x z\}_{i,j}^n.$$

4 Stability and well-balanced properties

This section aims at giving the stability and well-balanced properties of our schemes, and to discuss the use of limiters.

4.1 Positivity properties and discrete entropy inequality

Equipped with (25) and (26), we now aim at proving some stability properties of the scheme under some suitable CFL condition. We are especially interested in the case $\alpha = n+1-$ even though the first two lemmas stay valid for $\alpha = n$.

Lemma. *Under the CFL condition*

$$\frac{\Delta t}{\Delta x}\max_j \max_i \frac{1}{w_i}\left(\int_{\kappa_j} u(x,t^\alpha)\partial_x\Phi_{i,j}(x)\,\mathrm{d}x - \delta_{i,p}\left(u_{j+1/2}^{*,\alpha}\right)_- + \delta_{i,0}\left(u_{j-1/2}^{*,\alpha}\right)_+\right) < \frac{1}{2}, \tag{27}$$

the mean values $\overline{X}_j^{n+1}$, with $X = h, hu$, are convex combinations of the nodal values $\{X_{i,j}^{n+1-}\}_{i=0,\dots,p}$, $X_{0,j+1}^{n+1-}$ and $X_{p,j-1}^{n+1-}$. More precisely, we have

$$\begin{aligned}\overline{X}_j^{n+1} = \sum_{i=0}^p \left(\frac{w_i}{2} - \frac{\Delta t}{\Delta x}\left[\int_{\kappa_j} u(x,t^\alpha)\partial_x\Phi_{i,j}(x)dx - \delta_{i,p}\left(u_{j+1/2}^{*,\alpha}\right)_- + \delta_{i,0}\left(u_{j-1/2}^{*,\alpha}\right)_+\right]\right) X_{i,j}^{n+1-} \\ - \frac{\Delta t}{\Delta x}\left(u_{j+1/2}^{*,\alpha}\right)_- X_{0,j+1}^{n+1-} + \frac{\Delta t}{\Delta x}\left(u_{j-1/2}^{*,\alpha}\right)_+ X_{p,j-1}^{n+1-},\end{aligned} \tag{28}$$

where

$$\int_{\kappa_j} u(x,t^\alpha)\partial_x\Phi_{i,j}(x)dx = \frac{\Delta x}{2}\sum_{k=0}^p \omega_k u_{k,j}^\alpha \partial_x\Phi_{i,j}(x_{k,j}).$$

Proof. Let us multiply (24) by ω_i and sum over i. Setting $X = h, hu$, we immediately get

$$\overline{X}_j^{n+1} = \sum_{i=0}^p \frac{\omega_i}{2} L_{i,j}^\alpha X_{i,j}^{n+1-} - \frac{\Delta t}{\Delta x}\left[X_{j+1/2}^{*,n+1-} u_{j+1/2}^{*,\alpha} - X_{j-1/2}^{*,n+1-} u_{j-1/2}^{*,\alpha}\right].$$

Recall that $L_{i,j}^\alpha$ is given by (21) or equivalently

$$L_{i,j}^\alpha = \frac{2}{\omega_i}\left(\frac{\omega_i}{2} - \frac{\Delta t}{\Delta x}\left[\int_{\kappa_j} u^\alpha\,\partial_x\Phi_{i,j} - \delta_{i,p}\left(u_{j+1/2}^{*,\alpha}\right)_- + \delta_{i,0}\left(u_{j-1/2}^{*,\alpha}\right)_+\right]\right) \tag{29}$$

$$\delta_{i,p}\frac{\Delta t}{\Delta x}\left(u^{*,\alpha}_{j+1/2}\right)_+ - \delta_{i,0}\frac{\Delta t}{\Delta x}\left(u^{*,\alpha}_{j-1/2}\right)_-\Bigg).$$

Using the definition (23) of $X^{*,n+1-}_{j\pm1/2}$ easily gives (28). On the other hand, the coefficients in the combination (28) are non negative under the CFL condition (27) and since $\left(u^{*,\alpha}_{j+1/2}\right)_- \leq 0$ and $\left(u^{*,\alpha}_{j-1/2}\right)_+ \geq 0$. Finally, the sum of these coefficients equals one by (12) and (14).

As a consequence of this lemma, we can easily prove the following result which is concerned with the positivity of the water heights.

Lemma. *Under the CFL condition* (27)*, the quantities $L^\alpha_{i,j}$ are positive. Thus, if the water heights are positive at time t^n, that is to say if $h^n_{i,j} > 0$ for all i and j, then the water heights are also positive at the fictitious time t^{n+1-}, that is to say $h^{n+1-}_{i,j} > 0$ for all i and j, and the mean values are positive at time t^{n+1}, namely $\overline{h}^{n+1}_j > 0$ for all j.*

Proof. Under the CFL condition (27) and by (29), we have $L^\alpha_{i,j} > 0$. Since $L^\alpha_{i,j} h^{n+1-}_{i,j} = h^n_{i,j}$, it is thus clear that $h^{n+1-}_{i,j} > 0$ provided that $h^n_{i,j} > 0$. Finally, the mean values are positive by convex combination, which concludes the proof.

We now state that the proposed implicit explicit scheme satisfies a discrete entropy inequality. The proof is given in Appendix A.

Theorem. *Under the CFL condition* (27)*, the implicit explicit scheme (20) and (24) (or equivalently 25) with $\alpha = n+1-$ satisfies the following in-cell discrete non conservative entropy inequality which is consistent with (2), namely for all j*

$$\begin{aligned}(hE)(\overline{\boldsymbol{U}}^{n+1}_j) - \overline{(hE)}^n_j \\ + \frac{\Delta t}{\Delta x}\left[\left(\pi^{*,n+1-}_{j+1/2} + (hE)^{*,n+1-}_{j+1/2}\right)u^{*,n+1-}_{j+1/2} - \left(\pi^{*,n+1-}_{j-1/2} + (hE)^{*,n+1-}_{j-1/2}\right)u^{*,n+1-}_{j-1/2}\right] \\ \leq -\Delta t\,\{ghu\partial_x z\}^{n+1-}_j\,,\end{aligned}$$

where

$$\{ghu\partial_x z\}^{n+1-}_j = \sum_{i=0}^{p}\frac{\omega_i}{2}u^{n+1-}_{i,j}\{gh\partial_x z\}^n_{i,j} - \frac{1}{2a}\overleftarrow{W}^{n+1-}_{p,j}\{gh\partial_x z\}^n_{j+1/2} + \frac{1}{2a}\overrightarrow{W}^{n+1-}_{0,j}\{gh\partial_x z\}^n_{j-1/2}\,,$$

$$(hE)^{n+1-}_{j+1/2} = \begin{cases}(hE)^{n+1-}_{p,j} & \text{if} \quad u^*_{j+1/2} \geq 0,\\ (hE)^{n+1-}_{0,j+1} & \text{if} \quad u^*_{j+1/2} \leq 0,\end{cases}$$

and

$$\overrightarrow{W} = \Pi + au \quad \text{and} \quad \overleftarrow{W} = \Pi - au.$$

4.2 Well-balanced properties

We now give the well-balanced properties satisfied by our scheme. In the rest of this section, we assume that the initial condition satisfies the so-called lake at rest conditions, namely

$$u^0_{i,j} = 0 \quad \text{and} \quad h^0_{i,j} + z(x_{i,j}) = K$$

for all i and j and for a given constant K. We first state conditional well-balanced properties associated with the simple source term definition (19), and then give a new definition (30) which leads to unconditional well-balanced properties. These properties will be illustrated in the numerical section.

4.2.1 Conditional well-balanced properties

Our first result is concerned with the explicit explicit scheme, that is to say $\alpha = n$ in the Lagrangian step.

Proposition. *(i) Let us assume that the initial water height h^0 and the topography z are smooth polynomial functions of order less or equal than p. Then, the explicit explicit scheme ($\alpha = 0$) satisfies the well-balanced property for the mean values, that is to say*

$$\overline{u}_j^1 = 0 \quad \textit{and} \quad \overline{h}_j^1 + \overline{z}_j = K$$

for all j.
(ii) Let us assume that the initial water height h^0 and the topography z are smooth polynomial functions of order less or equal than $p/2$. Then, the explicit explicit scheme satisfies the well-balanced property for the nodal values, that is to say

$$u_{i,j}^1 = 0 \quad \textit{and} \quad h_{i,j}^1 + z(x_{i,j}) = K$$

for all j.

Proof. Let us begin with the mean values. By (16) with $\alpha = 0$, we clearly have $u_{j+1/2}^{*,0} = 0$ for all j (recall that $\Pi_{i,j}^0 = p_{i,j}^0 = p(h_{i,j}^0)$ for all i and j). On the other hand, (17) gives $\Pi_{j+1/2}^{*,0} = \Pi_{p,j}^0$ and $\Pi_{j-1/2}^{*,0} = \Pi_{0,j}^0$, and by (18) and the smoothness of z, $\{gh\partial_x z\}_{j\pm1/2}^0 = 0$. Therefore, (26) gives

$$\begin{cases} \overline{h}_j^1 = \overline{h}_j^0, \\ \overline{(hu)}_j^1 = \overline{(hu)}_j^0 - \dfrac{\Delta t}{\Delta x}\left[\Pi_{p,j}^0 - \Pi_{0,j}^0 + \Delta x \displaystyle\sum_{i=0}^{p} \frac{\omega_i}{2}\{gh\partial_x z\}_{i,j}^0\right]. \end{cases}$$

However, since $gh\partial_x z$ is a polynomial of order less than or equal to $2p-1$, we have

$$\Delta x \sum_{i=0}^{p} \frac{\omega_i}{2}\{gh\partial_x z\}_{i,j}^0 = \int_{\kappa_j} gh^0\partial_x z \,\mathrm{d}x = -\int_{\kappa_j} gh^0\partial_x h^0 \,\mathrm{d}x = 0 - \int_{\kappa_j} \partial_x \Pi^0 \,\mathrm{d}x = \Pi_{0,j}^0 - \Pi_{p,j}^0,$$

so that $\overline{h}_j^1 = \overline{h}_j^0$ and $\overline{(hu)}_j^1 = \overline{(hu)}_j^0$, which concludes the proof of (i). Let us now turn to the well-balanced property on the nodal values (ii). By (25), the same arguments as above give

$$\begin{cases} h_{i,j}^1 = h_{i,j}^0, \\ (hu)_{i,j}^1 = (hu)_{i,j}^0 - \dfrac{2\Delta t}{\omega_i \Delta x}\left[\delta_{i,p}\Pi_{p,j}^0 - \delta_{i,0}\Pi_{0,j}^0 - \dfrac{\Delta x}{2}\displaystyle\sum_{k=0}^{p} \omega_k \Pi_{k,j}^0 \partial_x \Phi_{i,j}(x_{k,j}) + \frac{\Delta x}{2}\omega_i\{gh^0\partial_x z\}_{i,j}^0\right]. \end{cases}$$

On the one hand, $gh\partial_x z$ is a polynomial of order less than or equal to $p-1$, so that we have that

$$\frac{\Delta x}{2}\omega_i\{gh^0\partial_x z\}_{i,j}^0 = \int_{\kappa_j} \Phi_{i,j} gh^0\partial_x z \,\mathrm{d}x.$$

On the other hand,

$$\begin{aligned}\frac{\Delta x}{2}\sum_{k=0}^{p}\omega_k\Pi^0_{k,j}\partial_x\Phi_{i,j}(x_{k,j}) - \frac{\Delta x}{2}\omega_i\{gh^0\partial_x z\}^0_{i,j} &= \int_{\kappa_j}\Pi^0_{k,j}\partial_x\Phi_{i,j}\,\mathrm{d}x - \int_{\kappa_j}\Phi_{i,j}gh^0\partial_x z\,\mathrm{d}x\\ &= \delta_{i,p}\Pi^0_{p,j} - \delta_{i,0}\Pi^0_{0,j} - \int_{\kappa_j}\Phi_{i,j}\partial_x\Pi^0_{k,j}\,\mathrm{d}x - \int_{\kappa_j}\Phi_{i,j}gh^0\partial_x z\,\mathrm{d}x\\ &= \delta_{i,p}\Pi^0_{p,j} - \delta_{i,0}\Pi^0_{0,j} - \int_{\kappa_j}\Phi_{i,j}\partial_x\Pi^0_{k,j}\,\mathrm{d}x + \int_{\kappa_j}\Phi_{i,j}\partial_x\Pi^0_{k,j}\,\mathrm{d}x\\ &= \delta_{i,p}\Pi^0_{p,j} - \delta_{i,0}\Pi^0_{0,j},\end{aligned}$$

which gives $(hu)^1_{i,j} = (hu)^0_{i,j}$ and concludes the proof.

The next result is concerned with the implicit explicit scheme.

Proposition. *Let us assume that the initial water height h^0 and the topography z are smooth polynomial functions of order less or equal than $p/2$. Then, the implicit explicit scheme ($\alpha = 1-$) satisfies the well-balanced property for the nodal values, that is to say*

$$u^1_{i,j} = 0 \quad \textit{and} \quad h^1_{i,j} + z(x_{i,j}) = K$$

for all j.

Proof. We first aim at checking that $h^{1-}_{i,j} = h^0_{i,j}$, $u^{1-}_{i,j} = u^0_{i,j}$ and $\Pi^{1-}_{i,j} = \Pi^0_{i,j}$ is the unique solution of (20) with $\alpha = n+1-$ (and $n = 0$). From (21), it is clear that $L^1_{i,j} = 1$ and (20) becomes

$$\begin{cases} 0 = 0\\ (hu)^{n+1-}_{i,j} = (hu)^n_{i,j} - \dfrac{2\Delta t}{\omega_i\Delta x}\left[\delta_{i,p}\Pi^n_{p,j} - \delta_{i,0}\Pi^n_{0,j} - \dfrac{\Delta x}{2}\displaystyle\sum_{k=0}^{p}\omega_k\Pi^n_{k,j}\partial_x\Phi_{i,j}(x_{k,j}) + \dfrac{\Delta x}{2}\omega_i\{gh^n\partial_x z\}^n_{i,j}\right],\\ 0 = 0. \end{cases}$$

The same arguments as in the proof of the previous Proposition also apply here to easily show that the second equality actually holds true. Then, the projection step is trivial since $L^1_{i,j} = 1$ and all the velocities are zero, which concludes the proof.

4.2.2 Unconditional well-balanced properties

As clearly stated in the above results, the well-balanced properties are subject to a restriction on the shapes of the initial water height and topography. It is actually possible to get rid of these restriction by simply changing the definition of the volume integral (19), as it was suggested to us by M. J. Castro. More precisely, if suffices to set

$$\{gh\partial_x z\}^n_{i,j} = gh^n_{i,j}\partial_x(h^n + z)(x_{i,j}) - g\partial_x\Pi^n(x_{i,j}). \tag{30}$$

The proof of this result follows the same lines as above and is left to the reader.

4.3 Positivity and generalized slope limiters

This section describes the limiters used to stabilize the proposed Discontinuous-Galerkin approach.

Positivity limiters. We have already proved the positivity of the nodal values $h^{n+1-}_{i,j}$ at the end of the Lagrange step and the mean values $\overline{h}^{n+1}_j$ at the end of the Projection step. Therefore and similarly

to [13], we use a positivity limiter to ensure that the nodal values $h_{i,j}^{n+1}$ are positive at the end of the Projection step. More precisely, we suggest to replace $h_{i,j}^{n+1}$ by $\theta_j h_{i,j}^{n+1} + (1-\theta_j)\,\overline{h}_j^{n+1}$, where the coefficients θ_j are taken to be

$$\theta_j = \min\left(1, \frac{\overline{h}_j^{n+1} - \varepsilon}{\overline{h}_j^{n+1} - \min_i h_{i,j}^{n+1}}\right).$$

This formula ensures that if h is less than a given threshold $\varepsilon > 0$, the nodal value of the corresponding cell is replaced by the positive mean value. In practice, ε is taken to be equal to 10^{-10}.

Generalized slope limiters in conservative variables. In order to avoid non physical oscillations, we also use the generalized slope limiters introduced in [9]. More precisely, considering the *minmod* function $m(a,b,c) = s \cdot \min(|a|,|b|,|c|)$ if $s = \text{sign}(a) = \text{sign}(b) = \text{sign}(c)$ and 0 otherwise, the increments

$$\Delta_+ \overline{X}_j^{n+1} = \overline{X}_{j+1}^{n+1} - \overline{X}_j^{n+1}, \quad \Delta_- \overline{X}_j^{n+1} = \overline{X}_j^{n+1} - \overline{X}_{j-1}^{n+1},$$

and the values

$$\begin{cases} X_{j+1/2}^{-,n+1} = \overline{X}_j^{n+1} + m\Big(X_{p,j}^{n+1} - \overline{X}_j^{n+1}, \Delta_+ \overline{X}_j^{n+1}, \Delta_- \overline{X}_j^{n+1}\Big), \\ X_{j-1/2}^{+,n+1} = \overline{X}_j^{n+1} - m\Big(\overline{X}_j^{n+1} - X_{0,j}^{n+1}, \Delta_+ \overline{X}_j^{n+1}, \Delta_- \overline{X}_j^{n+1}\Big), \end{cases}$$

the new states at time t^{n+1} are defined by

$$\begin{cases} X_{i,j}^{n+1} & \text{if } X_{j+1/2}^{-,n+1} = X_{p,j}^{n+1} \text{ and } X_{j-1/2}^{+,n+1} = X_{0,j}^{n+1}, \\ \overline{X}_j^{n+1} + \frac{2}{\Delta x}\,(x_{i,j} - x_j) \cdot m\Big(\partial_x X^{n+1}(x_j), \Delta_+ \overline{X}_j^{n+1}, \Delta_- \overline{X}_j^{n+1}\Big) & \text{otherwise.} \end{cases}$$

Generalized slope limiters in characteristic variables. As proposed in [16], one can also use the slope limiters written in characteristic variables. For each cell, instead of limiting on conservative variables $X = h$ or hu, we use the above general slope limiter on characteristic variables $\tilde{X} = W_1$ or W_2, where $W = R^{-1}\begin{pmatrix} h & hu \end{pmatrix}^T$. The matrix R is the one diagonalizing the Jacobian of the physical flux evaluated at the local mean values, namely

$$R^{-1} \frac{\partial f\big(\overline{U}\big)}{\partial U} R = \begin{pmatrix} \overline{u} + \overline{c} & 0 \\ 0 & \overline{u} - \overline{c} \end{pmatrix}$$

with $\overline{u} = \overline{q}/\overline{h}$, $\overline{c} = \sqrt{g\overline{h}}$,

$$\frac{\partial f\big(\overline{U}\big)}{\partial U} = \begin{pmatrix} 0 & 1 \\ g\overline{h} - \overline{u}^2 & 2\overline{u} \end{pmatrix} \qquad \text{and} \qquad R = \begin{pmatrix} 1 & 1 \\ \overline{u} + \overline{c} & \overline{u} - \overline{c} \end{pmatrix}.$$

We also take profit of the methodology proposed in [16] in order to keep the well-balanced property. We thus apply the general slope limiter on the local characteristic variables associated to $(h+z, q)$, instead of (h, q), on cells where the positivity limiter is not activated.

4.4 Time discretization

To conclude the description of our numerical strategy, let us briefly mention that the high order time discretization is obtained as in [13] using the Strong-Stability-Preserving Runge-Kutta approach, see [9]. For that, we consider the two steps of our Lagrange-Projection scheme as a single step which allows to define the solution at time t^{n+1} from the solution at time t^n.

5 Numerical results

The aim of this section is to illustrate the behaviour of our explicit-explicit and implicit-explicit Lagrange-Projection schemes, respectively denoted EXEX_p and IMEX_p, where p refers to the polynomial order of the DG approach. Recall that the sound speed is given by $c = \sqrt{p'(h)}$ with $p(h) = gh^2/2$ so that the parameter a is chosen locally at each interface according to

$$a_{j+1/2} = \kappa \max\left(h_j^n \sqrt{gh_j^n}, h_{j+1}^n \sqrt{gh_{j+1}^n}\right)$$

with $\kappa = 1.01$ and $g = 9.81$. We set $\Delta t = \min(\Delta t_{\text{Lag}}, \Delta t_{\text{Tra}})$ for the EXEX_p schemes and $\Delta t = \Delta t_{\text{Tra}}$ for the IMEX_p schemes where

$$\Delta t_{\text{Lag}} = \frac{\Delta x}{2p+1} \min_j \left(2a_{j+1/2} \min(\tau_{p,j}, \tau_{0,j+1})\right)$$

is the DG time-step restriction associated with the Lagrangian step, while the Transport step CFL restriction is taken from (27) to define Δt_{Tra}.

Comparison between limiters. In this test case, we first compare the results given by the general slope limiters applied to local conservative variables and characteristic variables. For that, we consider the simpler case of a constant topography, meaning that the source term is not taken into account. The space domain $[0, 1500]$ is divided into two parts with the same length and such that the total water height on the right-hand side is small compared to the left-hand side,

$$h(x, t = 0) = \begin{cases} 20, & \text{if } x \leq 750 \\ 1, & \text{if } x > 750. \end{cases}$$

The initial velocity is set to be zero on both sides and the final time is $T = 20$. At last, the spatial domain is discretized over a 500-cell uniform grid and absorbing (Neumann) boundary conditions are used.

We can observe on Figure 1 that the results of the EXEX_2 scheme with general slope limiters applied to local characteristic variables gives spurious oscillations in the rarefaction wave of a magnitude which is smaller than the one with general slope limiters applied to local conservative variables.

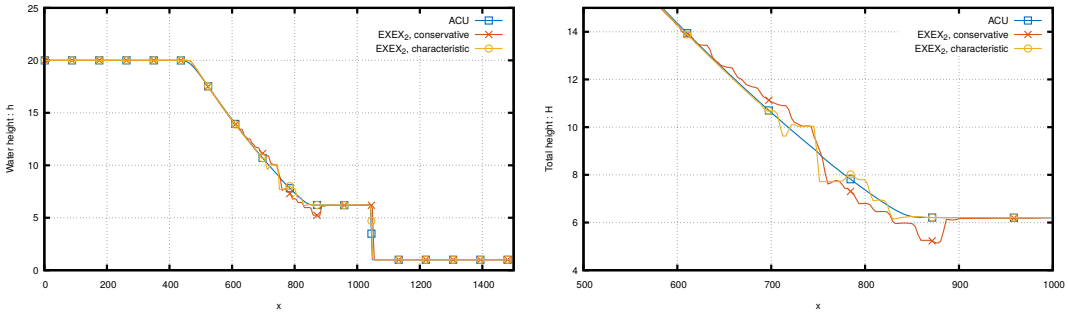

Figure 1: Comparison between general slope limiters applied on local conservative variables and characteristic variables at time $T = 20$, with a zoom around the oscillations on the right.

From now on, we will always use the general slope limiters applied to the characteristic variables.

Well-balanced property. The aim of this test case is to illustrate the theoretical results of Sections

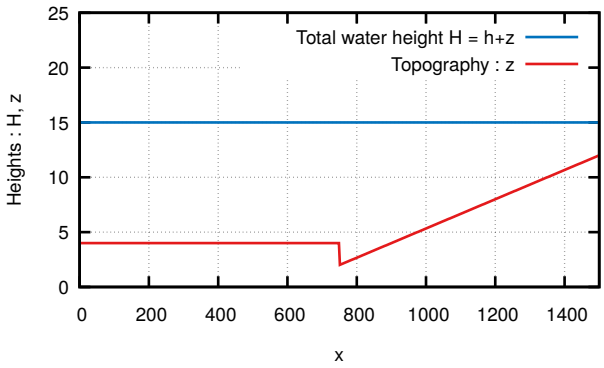

Figure 2: Well-balanced property, first-order polynomial topography and initial water height.

4.2.1 and 4.2.2 on the well-balanced properties of the EXEX and IMEX schemes, and both nodal and mean values. The initial velocity is set to be zero and the total water height is constant and equal to 15. The topography z is given by

$$z(x) = \begin{cases} 4, & \text{if } x \leq 750, \\ 2 + \frac{10}{750}\,(x - 750)\,, & \text{if } x > 750. \end{cases}$$

and represented on Figure 2. It is clearly discontinuous, constant on the left-hand side of the physical domain, and first-order polynomial of degree $r = 1$ on the right-hand side. As stated in Section 4.2.1, one can see in Table 1 that when considering the source term definition (19) the EXEX_1 scheme is exact for the mean values but not for nodal values, while the IMEX_1 scheme is not exact for both mean and nodal values. On the contrary, when $p \geq 2r = 2$, both EXEX_p and IMEX_p are exact for the mean and nodal values. Considering now the source term definition (30), one can recover the unconditional well-balanced property as clearly seen in Table 2 and according to Section 4.2.2.

In order to emphasize those results, we have run the same test case with now initial polynomials of degree $r = 2$ on the right-hand side. More precisely, the topography is now given by

$$z(x) = \begin{cases} 4, & \text{if } x \leq 750, \\ 2 + \frac{10}{750^2}\,(x - 750)^2\,, & \text{if } x > 750. \end{cases}$$

and is represented on Figure 3. The measure of the well-balanced properties are respectively given in Table 3 (Table 4) for source term definition (19) ((30)).

Note that in these test cases, we have used no limiters, although we observed that the use of general slope limiters compatible with the well-balanced property actually improves the results of the EXEX_p schemes when $p \leq 2r$.

Manufactured smooth solution. This test case is taken from [13] and allows us to test the experimental order of accuracy (EOA) of our schemes, especially on the Transport step. The space domain is $[0, 1]$, the boundary conditions are periodic and the initial conditions are $h_0(x) = 1+0.2\sin(2\pi x)$ and $u_0(x) = 1$. We solve (1) with a source term such that the exact solution is $h(x,t) = 1 + 0.2\sin(2\pi(x-t))$ and $u(x,t) = 1$, which just means that we impose $u_{i,j}^{n+1^-} = 1$ and $\Pi_{i,j}^{n+1^-} = \Pi_{i,j}^n$, so that the Acoustic step is trivial. For that reason we only present in this special case the results of EXEX_p schemes.

The EOA are reported in Table 5. We can observe that we have (at least) the correct $p + 1$ EOA.

Dam break problem. In this test case, we consider a classic dam break problem. We take the same kind of initial values as in the very first test case above, with velocity set to zero and total water height set

$r=1$		$T=\Delta t$, mean values		$T=\Delta t$, nodal values	
500-cell grid		$\|\overline{h+z}-15\|_\infty/15$	$\|\overline{q}/\overline{h}\|_\infty$	$\|h+z-15\|_\infty/15$	$\|q/h\|_\infty$
EXEX	$p=0$	9.88 E−17	0.00 E−17	9.88 E−17	0.00 E−17
	$p=1$	**9.88 E−17**	**4.49 E−16**	9.87 E−17	**9.75 E−6**
	$p=2$	1.98 E−16	0.00 E−17	9.87 E−17	0.00 E−17
	$p=3$	1.98 E−16	0.00 E−17	9.87 E−17	0.00 E−17
IMEX	$p=0$	9.88 E−17	0.00 E−17	9.88 E−17	0.00 E−17
	$p=1$	**4.91 E−7**	**9.92 E−6**	8.37 E−7	**4.86 E−5**
	$p=2$	1.98 E−16	0.00 E−17	9.87 E−17	0.00 E−17
	$p=3$	1.98 E−16	0.00 E−17	9.87 E−17	0.00 E−17

Table 1: Measure of the well-balanced property associated with initial h and z given on Figure 2 and source term definition (19).

$r=1$		$T=\Delta t$, mean values		$T=\Delta t$, nodal values	
500-cell grid		$\|\overline{h+z}-15\|_\infty/15$	$\|\overline{q}/\overline{h}\|_\infty$	$\|h+z-15\|_\infty/15$	$\|q/h\|_\infty$
EXEX	$p=0$	9.88 E−17	0.00 E−17	9.88 E−17	0.00 E−17
	$p=1$	**9.88 E−17**	**0.00 E−17**	9.87 E−17	**0.00 E−17**
	$p=2$	1.98 E−16	0.00 E−17	9.87 E−17	0.00 E−17
	$p=3$	1.98 E−16	0.00 E−17	9.87 E−17	0.00 E−17
IMEX	$p=0$	9.88 E−17	0.00 E−17	9.88 E−17	0.00 E−17
	$p=1$	**9.88 E−17**	**0.00 E−17**	9.87 E−17	**0.00 E−17**
	$p=2$	1.98 E−16	0.00 E−17	9.87 E−17	0.00 E−17
	$p=3$	1.98 E−16	0.00 E−17	9.87 E−17	0.00 E−17

Table 2: Measure of the well-balanced property associated with initial h and z given on Figure 2 and source term definition (30).

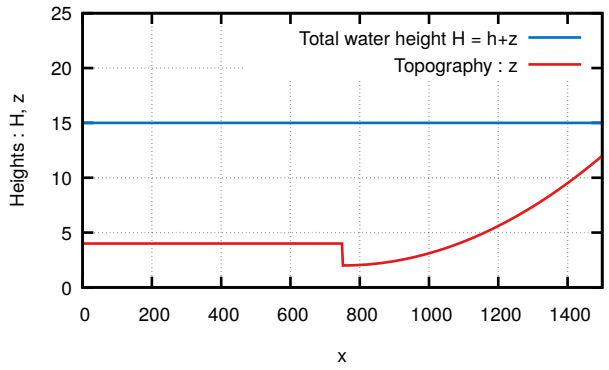

Figure 3: Well-balanced property, second-order polynomial topography and initial water height.

$r=2$		$T=\Delta t$, mean values		$T=\Delta t$, nodal values	
500-cell grid		$\|\overline{h+z}-15\|_\infty/15$	$\|\overline{q}/\overline{h}\|_\infty$	$\|h+z-15\|_\infty/15$	$\|q/h\|_\infty$
EXEX	$p=0$	9.87 E−17	0.00 E−17	9.87 E−17	0.00 E−17
	$p=1$	9.87 E−17	4.47 E−16	9.87 E−17	**3.88 E−5**
	$p=2$	**1.97 E−16**	**3.05 E−16**	9.87 E−17	**4.67 E−8**
	$p=3$	**1.97 E−16**	**2.63 E−16**	9.87 E−17	**1.34 E−11**
	$p=4$	1.98 E−16	0.00 E−17	9.87 E−17	0.00 E−17
IMEX	$p=0$	9.87 E−17	0.00 E−17	9.87 E−17	0.00 E−17
	$p=1$	**1.97 E−6**	**3.89 E−5**	2.67 E−6	**1.93 E−4**
	$p=2$	**4.70 E−10**	**9.74 E−9**	6.83 E−9	**1.72 E−7**
	$p=3$	**3.45 E−14**	**6.86 E−13**	1.78 E−12	**3.97 E−11**
	$p=4$	1.98 E−16	0.00 E−17	9.87 E−17	0.00 E−17

Table 3: Measure of the well-balanced property associated with initial h and z given on Figure 3 and source term definition (19).

$r=2$		$T=\Delta t$, mean values		$T=\Delta t$, nodal values	
500-cell grid		$\|\overline{h+z}-15\|_\infty/15$	$\|\overline{q}/\overline{h}\|_\infty$	$\|h+z-15\|_\infty/15$	$\|q/h\|_\infty$
EXEX	$p=0$	9.87 E−17	0.00 E−17	9.87 E−17	0.00 E−17
	$p=1$	9.87 E−17	0.00 E−17	9.87 E−17	**0.00 E−17**
	$p=2$	**1.97 E−16**	**0.00 E−17**	9.87 E−17	**0.00 E−17**
	$p=3$	**1.97 E−16**	**0.00 E−17**	9.87 E−17	**0.00 E−17**
	$p=4$	1.97 E−16	0.00 E−17	9.87 E−17	0.00 E−17
IMEX	$p=0$	9.87 E−17	0.00 E−17	9.87 E−17	0.00 E−17
	$p=1$	**9.87 E−17**	**0.00 E−17**	9.87 E−17	**0.00 E−17**
	$p=2$	**1.97 E−16**	**0.00 E−17**	9.87 E−17	**0.00 E−17**
	$p=3$	**1.97 E−16**	**0.00 E−17**	9.87 E−17	**0.00 E−17**
	$p=4$	1.97 E−16	0.00 E−17	9.87 E−17	0.00 E−17

Table 4: Measure of the well-balanced property associated with initial h and z given on Figure 3 and source term definition (30).

Δx	$p=0$		$p=1$		$p=2$	
	L^1-error	EOA	L^1-error	EOA	L^1-error	EOA
1/64	5.79E-02		6.46E-04		9.30E-08	
1/128	3.34E-02	0.792118	1.62E-04	1.996037	6.48E-09	3.843292
1/256	1.80E-02	0.889836	4.05E-05	1.998163	4.23E-10	3.936130
1/512	9.39E-03	0.943063	1.01E-05	1.999183	2.72E-11	3.959514

Table 5: EOA for the manufactured smooth solution at time $T = 0.5$, L^1-error $= {}^{\|h-h^{\mathrm{Ex}}\|_1}/_{\|h^{\mathrm{Ex}}\|_1}$.

to

$$H(x, t=0) = h(x, t=0) + z(x) = \begin{cases} 20, & \text{if } x \leq 750 \\ 15, & \text{if } x > 750. \end{cases}$$

However, the topography is not flat but given by the regularized two-step function

$$z(x) = \begin{cases} 4e^{2-\frac{150}{x-487.5}}, & \text{if } 487.5 < x <= 562.5, \\ 8 - 4e^{2-\frac{150}{637.5-x}}, & \text{if } 562.5 < x <= 637.5, \\ 8, & \text{if } 637.5 < x <= 862.5, \\ 8 - 4e^{2-\frac{150}{x-862.5}}, & \text{if } 862.5 < x <= 937.5, \\ 4e^{2-\frac{150}{1012.5-x}}, & \text{if } 937.5 < x <= 1012.5, \\ 0 & \text{otherwise.} \end{cases}$$

At last, the spatial domain is discretized over a 1500-cell grid and we keep the absorbing boundary conditions.

We can observe the results on Figure 4 for EXEX_p schemes on the left column and IMEX_p schemes on the right one. The top graphs represents the topography and total water heights at final time $T = 50$. A zoom of the shock moving towards the right boundary is given in the middle graphs. We can see here the expected diffusivity of the IMEX_p schemes although the slope becomes stiffer as the order grows. This last remark can be also done for the EXEX_p schemes. Finally the last graphs represents the velocities. We also show on these graphs the results given by the so-denoted ACU scheme derived in [1].

Propagation of perturbations. This test case focuses on the perturbation of a steady state solution by a pulse that splits into two opposite waves. More precisely, the space domain is reduced to the interval $[0, 2]$, the bottom topography is defined by $z(x) = 2 + 0.25(\cos(10\pi(x - 0.5)) + 1)$ if $1.4 < x < 1.6$, and 2 otherwise, and the initial state is such that $u(0, x) = 0$ and $h(0, x) = 3 - z(x) + \Delta h$ if $1.1 < x < 1.2$, and $3 - z(x)$ otherwise, where $\Delta h = 0.001$ is the height of the perturbation. The CFL parameter is set to 0.9, the final time is $T = 0.2$, the space step equals $\Delta x = 1/500$ and Neumann boundary conditions are used.

It turns out that since the perturbation is small, the values of the velocity u keeps a small amplitude during the whole computation. As an immediate consequence, considering the natural implicit-explicit CFL condition gives very large time steps which naturally induces much numerical diffusion. In order to reduce the numerical diffusion and improve the overall accuracy of the numerical solution, the time step is taken as $\Delta t = \min\left(10\Delta t_{\mathrm{Lag}}, \Delta t_{\mathrm{Tra}}\right)$ for the IMEX_p schemes.

Figure 5 compares the numerical solutions given by the EXEX_p, IMEX_p and ACU schemes. The implicit-explicit schemes are clearly more diffusive than the full explicit ones. Thought in both explicit and implicit schemes we denote an improvement when p gets larger.

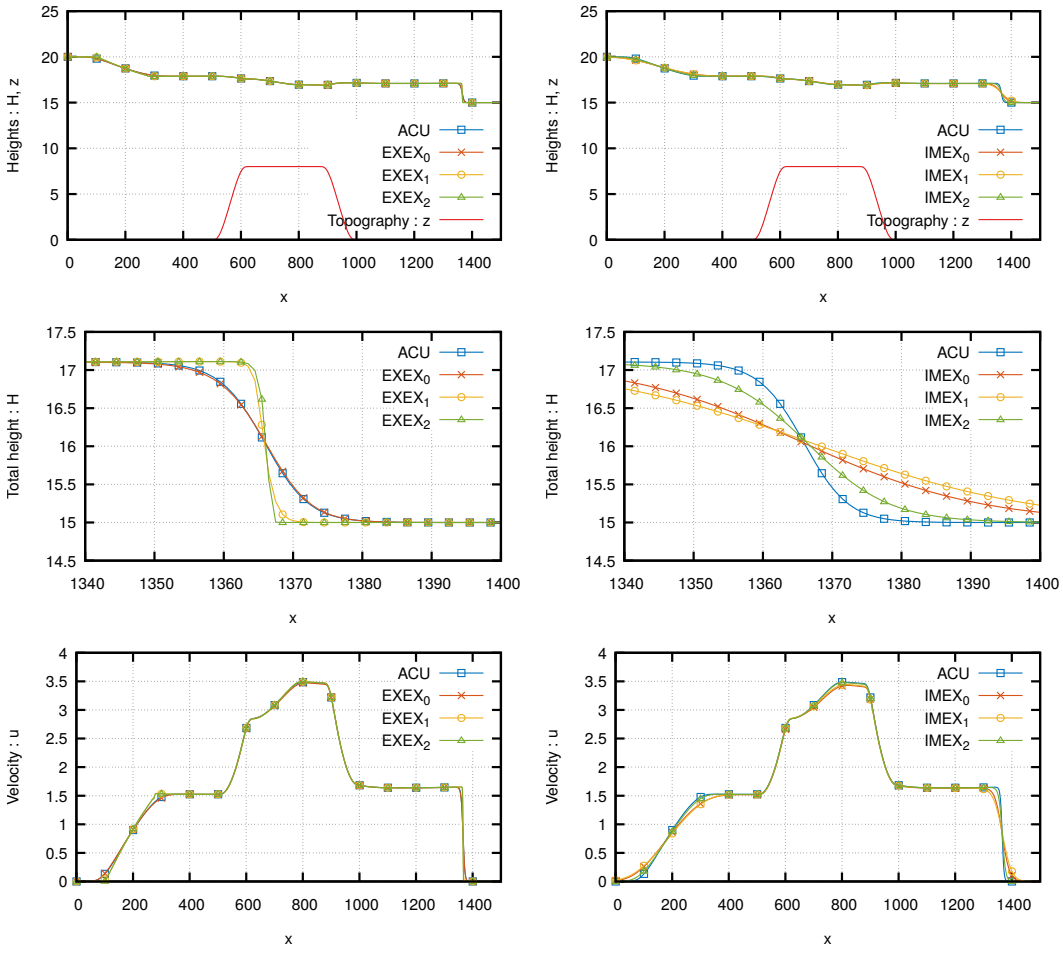

Figure 4: Dam break problem, topography and total water heights (top and middle) and velocity (bottom) at time $T = 50$, EXEX$_p$ (left), IMEX$_p$ (right).

Fluvial regime. The aim of this test case is to test the ability of the schemes to converge to some moving water equilibrium. Let us remind that the steady states are governed by the equations $hu = K_1$ and $\frac{u^2}{2} + g(h + z) = K_2$, and we denote $h_{eq}(x), u_{eq}(x)$ the values of h and u at this equilibrium. In this fluvial case we set $K_1 = 1$ and $K_2 = 25$. The domain is $[0, 4]$ and the bottom topography is defined by $z(x) = (\cos(10\pi(x - 1)) + 1)/4$ if $1.9 \leq x \leq 2.1$ and 0 elsewhere. The CFL parameter is equal to 0.5 and the space step to $\Delta x = 1/400$. The initial condition is chosen out of equilibrium and given by $h = h_{eq}$ and $u = 0$. The boundary conditions are set to be

$$\begin{cases} \partial_x h(x = 0) = 0, \\ (hu)(x = 0) = K_1, \end{cases} \quad \text{and} \quad \begin{cases} h(x = 4) = h_{eq}(x = 4), \\ \partial_x (hu)(x = 4) = 0. \end{cases}$$

Figure 6 shows the solution at the final time $t = 50$. We can observe that the solutions are close to the expected equilibrium, except near the mid domain where the momentum is not yet constant for the mesh size under consideration. Finally, the solutions are more accurate for both EXEX and IMEX schemes when the order grows.

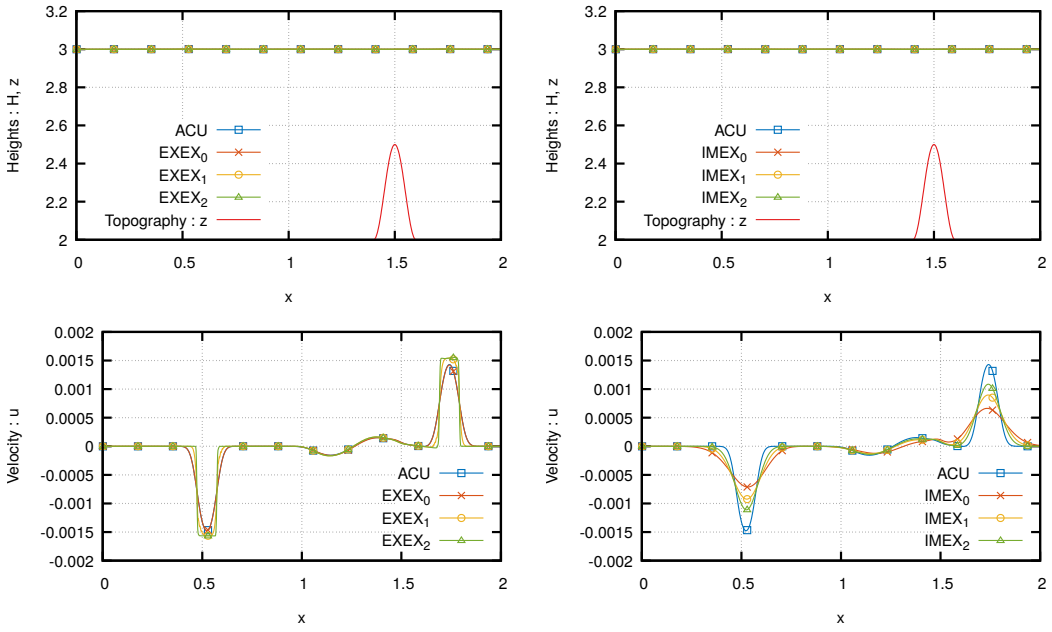

Figure 5: Propagation of perturbation problem, topography and total water heights (top) and velocity (bottom) at time $T = 0.2$, EXEX_p (left), IMEX_p (right).

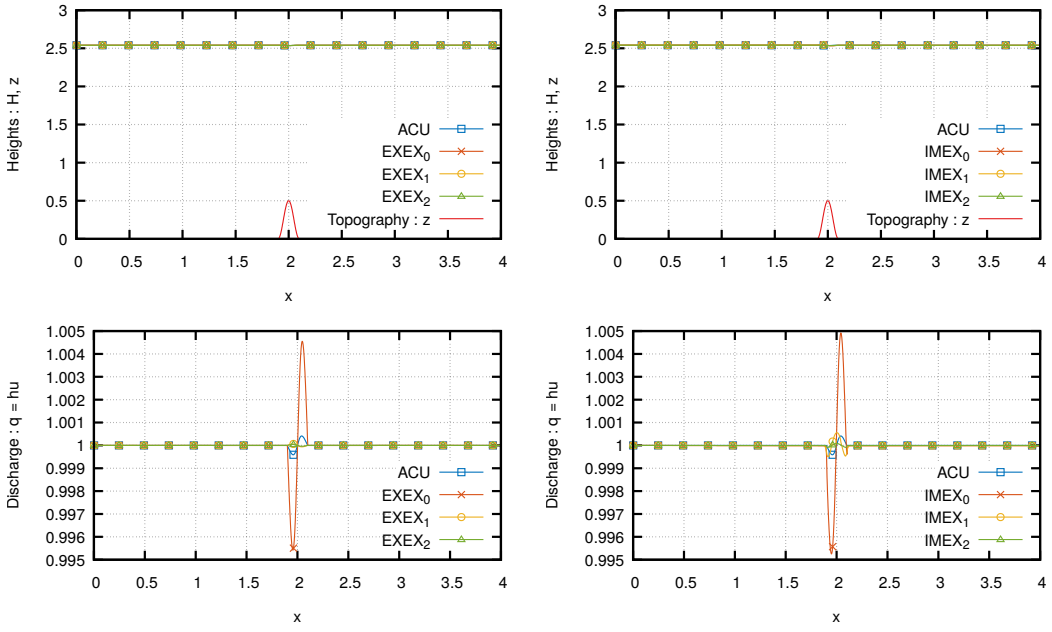

Figure 6: Fluvial regime at time $T = 200$. On top : total heights $h + z$, on bottom : discharge hu, respectively for EXEX_p (IMEX_p) on the left (right).

Transcritical regime without shock. In this test case, we take the same framework as in the fluvial test case above but we set $K_1 = 3$, $K_2 = \frac{3}{2}(K_1 g)^{2/3} + \frac{g}{2}$. The solutions of IMEX schemes are shown at time $T = 10$ on Figure 7 and here again the accuracy gets better when the order grows. The solutions of EXEX schemes are not given since the limiters are not able to subside the spurious oscillations on this test case.

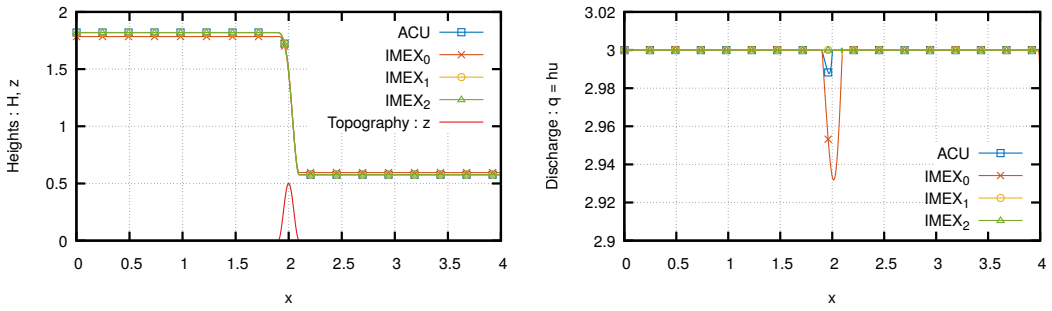

Figure 7: Transcritical regime without shock. On the left : total heights $h + z$, on the right : discharge hu.

Transcritical regime with shock : This test has been proposed by Castro et al. [3]. The parameters are described hereafter: the space domain is the interval $[0, 25]$, the bottom topography is defined by $z(x) = 3 - 0.005(x - 10)^2$, if $8 < x < 12$, and 2.8 otherwise. The initial state is defined by $h(0, x) = 3.13 - z(x)$, $q(0, x) = 0.18$ and the boundary conditions are $q(t, 0) = 0.18$, $\partial_x q(t, 25) = 0$, $h(t, 25) = 0.33$ and $\partial_x h(t, 0) = 0$. The final time is set to $T = 200$, the space step to $\Delta x = 1/64$ and the CFL to 0.9. We can see on Figure 8 that the total water height is properly computed while the limiters are not able to reasonably control the spurious oscillations (note however that an overshoot is already present with the first-order finite volume ACU scheme).

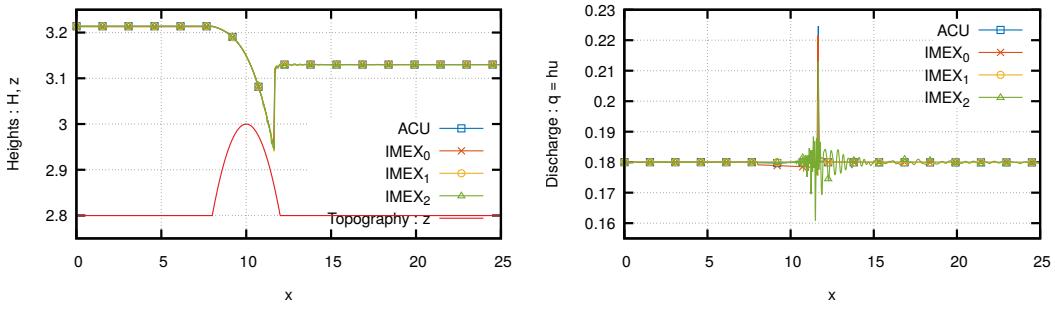

Figure 8: Transcritical regime with shock at final time $T = 200$. On the left : total heights $h + z$, on the right : discharge hu.

Acknowledgement. The authors are very grateful to P. Kestener, S. Kokh and F. Renac for stimulating discussions, and the "Maison de la Simulation" for providing excellent working conditions to the second author. The authors are also very grateful to M. J. Castro for providing us with the definition (30) of the source term volume integral leading to the validity of the unconditional well-balanced prop-

erty with no restriction on the shape of the initial water height and topography (see Section 4.2.2). The first author was partially funded by ANR Achylles (grant ANR-14-CE25-0001-03).

References

[1] E. Audusse, C. Chalons, and P. Ung. A very simple well-balanced positive and entropy-satisfying scheme for the shallow-water equations. *Communications in Mathematical Sciences*, 5(13):1317–1332, 2015.

[2] F. Bouchut. Nonlinear stability of finite volume methods for hyperbolic conservation laws, and well-balanced schemes for sources. *Frontiers in Mathematics series, Birkhäuser*, 2004.

[3] M. J. Castro, A. Pardo Milanés, and C. Parés. Well-balanced numerical schemes based on a generalized hydrostatic reconstruction technique. *Mathematical Models and Methods in Applied Sciences*, 17(12):2055–2113, 2007.

[4] C. Chalons, M. Girardin, and S. Kokh. Large time step and asymptotic preserving numerical schemes for the gas dynamics equations with source terms. *SIAM Journal of Scientific Computing*, 35(6):2874–2902, 2013.

[5] C. Chalons, M. Girardin, and S. Kokh. An all-regime lagrange-projection like scheme for the gas dynamics equations on unstructured meshes. *Communications in Computational Physics*, 20(1):188–233, 2016.

[6] C. Chalons, M. Girardin, and S. Kokh. An all-regime lagrange-projection like scheme for 2d homogeneous models for two-phase flows on unstructured meshes. *Journal of Computational Physics*, 335:885–904, 2017.

[7] C. Chalons, P. Kestener, S. Kokh, and M. Stauffert. A large time-step and well-balanced lagrange-projection type scheme for the shallow-water equations. *Communications in Mathematical Sciences*, 15(3):765–788, 2017.

[8] C. Chalons and M. Stauffert. A high-order discontinuous galerkin lagrange projection scheme for the barotropic euler equations. *Proceedings of the 2017 FVCA8 international conference on Finite Volumes for Complex Applications*, 2017.

[9] B. Cockburn and C.-W. Shu. Runge–kutta discontinuous galerkin methods for convection-dominated problems. *Journal of scientific computing*, 16(3):173–261, 2001.

[10] F Coquel, Q.L. Nguyen, M. Postel, and Q.H. Tran. Entropy-satisfying relaxation method with large time-steps for euler ibvps. *Mathematics of Computation*, 79:1493–1533, 2010.

[11] L. Gosse. Computing qualitatively correct approximations of balance laws. exponential-fit, well-balanced and asymptotic-preserving. *SEMA SIMAI Springer Series 2*, 2013.

[12] S Jin and Z. P. Xin. The relaxation schemes for systems of conservation laws in arbitrary space dimension. *Comm. Pure Appl. Math.*, 48(3):235–276, 1995.

[13] F. Renac. A robust high-order lagrange-projection like scheme with large time steps for the isentropic euler equations. *Numerische Mathematik*, pages 1–27, 2016.

[14] C.-W. Shu and S. Osher. Efficient implementation of essentially non-oscillatory shock-capturing schemes. *Journal of Computational Physics*, 77(2):439–471, 1988.

[15] I. Suliciu. On the thermodynamics of fluids with relaxation and phase transitions. fluids with relaxation. *Int. J. Engag. Sci.*, 36:921–947, 1998.

[16] Y. Xing, X. Zhang, and C.-W. Shu. Positivity-preserving high order well-balanced discontinuous galerkin methods for the shallow water equations. *Advances in Water Resources*, 33(12):1476–1493, 2010.

A Proof of the discrete entropy inequality

We adapt the proof given in [7] for the first order finite volume implicit explicit Lagrange Projection scheme to the present Discontinuous Galerkin setting.

The acoustic step. Let us first introduce the characteristic variables

$$\overrightarrow{W} = \Pi + au \quad \text{and} \quad \overleftarrow{W} = \Pi - au.$$

Thanks to (20) and using an integration by part to equivalently replace the quadrature formula of $\int \overrightarrow{W}\partial_x\Phi dx$ by the one of $\int \partial_x(\overrightarrow{W}\Phi)dx - \int \Phi\partial_x\overrightarrow{W}dx$, we easily get

$$\begin{aligned}
\overrightarrow{W}_{i,j}^{n+1-} = \overrightarrow{W}_{i,j}^{n} - a\frac{2\Delta t}{\omega_i\Delta x}\tau_{i,j}^n\Bigg[&\delta_{i,p}\left(\overrightarrow{W}_{p,j}^{n+1-} - \frac{\Delta x}{2}\left\{gh\partial_x z\right\}_{j+1/2}\right)\\
&- \delta_{i,0}\left(\overrightarrow{W}_{p,j-1}^{n+1-} - \frac{\Delta x}{2}\left\{gh\partial_x z\right\}_{j-1/2}\right)\\
&- \frac{\Delta x}{2}\sum_{k=0}^{p}\omega_k\overrightarrow{W}_{k,j}^{n+1-}\partial_x\phi_{i,j}(x_{k,j})\Bigg]\\
- a\,\Delta t\,\tau_{i,j}^n&\left[\frac{\delta_{i,p}}{\omega_p}\{gh\partial_x z\}_{j+1/2}^n + \frac{\delta_{i,0}}{\omega_0}\{gh\partial_x z\}_{j-1/2}^n + \{gh\partial_x z\}_{i,j}^n\right]\\
= \overrightarrow{W}_{i,j}^{n} - a\frac{2\Delta t}{\omega_i\Delta x}\tau_{i,j}^n\Bigg[&\frac{\Delta x}{2}\omega_i\left(\partial_x\overrightarrow{W}|_{i,j}^{n+1-} + \{gh\partial_x z\}_{i,j}^n\right)\\
&+ \delta_{i,0}\left(\overrightarrow{W}_{0,j}^{n+1-} - \overrightarrow{W}_{p,j-1}^{n+1-} + \Delta x\left\{gh\partial_x z\right\}_{j-1/2}^n\right)\Bigg],
\end{aligned}$$

and similarly

$$\begin{aligned}
\overleftarrow{W}_{i,j}^{n+1-} = \overleftarrow{W}_{i,j}^{n} + a\frac{2\Delta t}{\omega_i\Delta x}\tau_{i,j}^n\Bigg[&\frac{\Delta x}{2}\omega_i\left(\partial_x\overleftarrow{W}|_{i,j}^{n+1-} + \{gh\partial_x z\}_{i,j}^n\right)\\
&+ \delta_{i,p}\left(\overleftarrow{W}_{0,j+1}^{n+1-} - \overleftarrow{W}_{p,j}^{n+1-} + \Delta x\left\{gh\partial_x z\right\}_{j+1/2}^n\right)\Bigg].
\end{aligned}$$

We then multiply the first equation by $\overrightarrow{W}_{i,j}^{n+1-}$ and the second one by $\overleftarrow{W}_{i,j}^{n+1-}$ to obtain

$$\begin{aligned}
\overrightarrow{W}_{i,j}^{n+1-}\left(\overrightarrow{W}_{i,j}^{n+1-} - \overrightarrow{W}_{i,j}^{n}\right) = -a\frac{2\Delta t}{\omega_i\Delta x}\tau_{i,j}^n\Bigg[&\frac{\Delta x}{2}\omega_i\left(\partial_x\frac{\overrightarrow{W}^2}{2}|_{i,j}^{n+1-} + \overrightarrow{W}_{i,j}^{n+1-}\{gh\partial_x z\}_{i,j}^n\right)\\
&+ \delta_{i,0}\overrightarrow{W}_{0,j}^{n+1-}\left(\overrightarrow{W}_{0,j}^{n+1-} - \overrightarrow{W}_{p,j-1}^{n+1-} + \Delta x\left\{gh\partial_x z\right\}_{j-1/2}^n\right)\Bigg],
\end{aligned}$$

and

$$\begin{aligned}
\overleftarrow{W}_{i,j}^{n+1-}\left(\overleftarrow{W}_{i,j}^{n+1-} - \overleftarrow{W}_{i,j}^{n}\right) = a\frac{2\Delta t}{\omega_i\Delta x}\tau_{i,j}^n\Bigg[&\frac{\Delta x}{2}\omega_i\left(\partial_x\frac{\overleftarrow{W}^2}{2}|_{i,j}^{n+1-} + \overleftarrow{W}_{i,j}^{n+1-}\{gh\partial_x z\}_{i,j}^n\right)\\
&+ \delta_{i,p}\overleftarrow{W}_{p,j}^{n+1-}\left(\overleftarrow{W}_{0,j+1}^{n+1-} - \overleftarrow{W}_{p,j}^{n+1-} + \Delta x\left\{gh\partial_x z\right\}_{j+1/2}^n\right)\Bigg].
\end{aligned}$$

Using the identities $2b(b-a) = (b^2-a^2) + (a-b)^2$ and $2a(b-a) = (b^2-a^2) - (b-a)^2$, we easily get

$$(\overrightarrow{W}_{i,j}^{n+1-})^2 - (\overrightarrow{W}_{i,j}^{n})^2 + a\frac{2\Delta t}{\omega_i \Delta x}\tau_{i,j}^n \left[\frac{\Delta x}{2}\omega_i \partial_x \overrightarrow{W}^2|_{i,j}^{n+1-} + \delta_{i,0}\left((\overrightarrow{W}_{0,j}^{n+1-})^2 - (\overrightarrow{W}_{p,j-1}^{n+1-})^2\right)\right]$$
$$\leq -2a\frac{2\Delta t}{\omega_i \Delta x}\tau_{i,j}^n \left[\frac{\Delta x}{2}\omega_i \overrightarrow{W}_{i,j}^{n+1-}\{gh\partial_x z\}_{i,j}^n + \delta_{i,0}\overrightarrow{W}_{0,j}^{n+1-}\Delta x\,\{gh\partial_x z\}_{j-1/2}^n\right],$$

and

$$(\overleftarrow{W}_{i,j}^{n+1-})^2 - (\overleftarrow{W}_{i,j}^{n})^2 - a\frac{2\Delta t}{\omega_i \Delta x}\tau_{i,j}^n \left[\frac{\Delta x}{2}\omega_i \partial_x \overleftarrow{W}^2|_{i,j}^{n+1-} + \delta_{i,p}\left((\overleftarrow{W}_{0,j+1}^{n+1-})^2 - (\overleftarrow{W}_{p,j}^{n+1-})^2\right)\right]$$
$$\leq 2a\frac{2\Delta t}{\omega_i \Delta x}\tau_{i,j}^n \left[\frac{\Delta x}{2}\omega_i \overleftarrow{W}_{i,j}^{n+1-}\{gh\partial_x z\}_{i,j}^n + \delta_{i,p}\overleftarrow{W}_{p,j}^{n+1-}\Delta x\,\{gh\partial_x z\}_{j+1/2}^n\right].$$

Note now that

$$\frac{\overrightarrow{W}^2 + \overleftarrow{W}^2}{2} = \Pi^2 + a^2u^2 \quad \text{and} \quad \frac{\overrightarrow{W}^2 - \overleftarrow{W}^2}{2} = 2au\Pi.$$

Therefore, setting

$$\eta = \frac{\overrightarrow{W}^2 + \overleftarrow{W}^2}{2}$$

and summing the two inequalities above leads to

$$\eta_{i,j}^{n+1-} - \eta_{i,j}^n + 2a^2\frac{2\Delta t}{\omega_i \Delta x}\tau_{i,j}^n\Big[\frac{\Delta x}{2}\omega_i \partial_x(\Pi u)|_{i,j}^{n+1-}$$
$$- \frac{\delta_{i,p}}{4a}\left((\overleftarrow{W}_{0,j+1}^{n+1-})^2 - (\overleftarrow{W}_{p,j}^{n+1-})^2\right) + \frac{\delta_{i,0}}{4a}\left((\overrightarrow{W}_{0,j}^{n+1-})^2 + (\overrightarrow{W}_{p,j-1}^{n+1-})^2\right)\Big]$$
$$\leq -2a^2\frac{2\Delta t}{\omega_i \Delta x}\tau_{i,j}^n\Big[\frac{\Delta x}{2}\omega_i u_{i,j}^{n+1-}\{gh\partial_x z\}_{i,j}^n$$
$$- \frac{\delta_{i,p}}{2a}\overleftarrow{W}_{p,j}^{n+1-}\Delta x\,\{gh\partial_x z\}_{j+1/2}^n + \frac{\delta_{i,0}}{2a}\overrightarrow{W}_{0,j}^{n+1-}\Delta x\,\{gh\partial_x z\}_{j-1/2}^n\Big]. \quad (31)$$

With a little abuse in the notations, let us now consider the internal energy e and the pressure p as functions of $\tau = 1/h$, so that $e(\tau) = g/2\tau$ and $e'(\tau) = -p(\tau)$, while the total energy E is still given by $E = u^2/2 + e$. Since

$$E - \frac{\eta}{2a^2} = e + \frac{\Pi^2}{2a^2}$$

and

$$\Pi_{i,j}^{n+1-} - \Pi_{i,j}^n = -a^2(\tau_{i,j}^{n+1-} - \tau_{i,j}^n)$$

by (15), we thus have

$$E_{i,j}^{n+1-} - E_{i,j}^n - \frac{\eta_{i,j}^{n+1-} - \eta_{i,j}^n}{2a^2} = e(\tau_{i,j}^{n+1-}) - e(\tau_{i,j}^n) - \frac{(\Pi_{i,j}^{n+1-} - \Pi_{i,j}^n)^2}{2a^2} - \frac{\Pi_{i,j}^n(\Pi_{i,j}^{n+1-} - \Pi_{i,j}^n)}{a^2}$$
$$= e(\tau_{i,j}^{n+1-}) - e(\tau_{i,j}^n) + \Pi_{i,j}^n(\tau_{i,j}^{n+1-} - \tau_{i,j}^n) - \frac{a^2}{2}(\tau_{i,j}^{n+1-} - \tau_{i,j}^n)^2$$
$$= \frac{(e^{''}(\xi) - a^2)}{2}(\tau_{i,j}^{n+1-} - \tau_{i,j}^n)^2$$

for some ξ in between $\tau_{i,j}^n$ and $\tau_{i,j}^{n+1-}$. Note that $e''(\xi) = -p'(\xi)$ so that under the sub-characteristic condition

$$a > \max_j \max_{\tau \in \mathcal{I}(\tau_{i,j}^n, \tau_{i,j}^{n+1-})} \sqrt{-p'(\tau)},$$

we have

$$E_{i,j}^{n+1-} - E_{i,j}^{n} - \frac{\eta_{i,j}^{n+1-} - \eta_{i,j}^{n}}{2a^2} \leq 0.$$

Multiplying this inequality by $h_{i,j}^n = L_{i,j}^{n+1-} h_{i,j}^{n+1-}$, we get

$$(hE)_{i,j}^{n+1-} - (hE)_{i,j}^{n} + \left(L_{i,j}^{n+1-} - 1\right)(hE)_{i,j}^{n+1-} - h_{i,j}^{n} \frac{\eta_{i,j}^{n+1-} - \eta_{i,j}^{n}}{2a^2} \leq 0.$$

We are now ready to establish the energy mean value inequality. Multiplying the last inequality by $\omega_i/2$, summing over i and using (31) leads to

$$\begin{aligned}
&\overline{(hE)}_j^{n+1-} - \overline{(hE)}_j^{n} + \sum_{i=0}^{p} \frac{\omega_i}{2} \left(L_{i,j}^{n+1-} - 1\right)(hE)_{i,j}^{n+1-} \\
&+ \frac{\Delta t}{\Delta x} \left[\int_{\kappa_j} \partial_x (\Pi u)(x, t^{n+1-}) dx - \frac{1}{4a} \left((\overleftarrow{W}_{0,j+1}^{n+1-})^2 - (\overleftarrow{W}_{p,j}^{n+1-})^2 \right) + \frac{1}{4a} \left((\overrightarrow{W}_{0,j}^{n+1-})^2 - (\overrightarrow{W}_{p,j-1}^{n+1-})^2 \right) \right] \\
&\qquad \leq -\Delta t \, \{ghu\partial_x z\}_j^{n+1-},
\end{aligned}$$

where we have set

$$\{ghu\partial_x z\}_j^{n+1-} = \sum_{i=0}^{p} \frac{\omega_i}{2} u_{i,j}^{n+1-} \{gh\partial_x z\}_{i,j}^{n} - \frac{1}{2a} \overleftarrow{W}_{p,j}^{n+1-} \{gh\partial_x z\}_{j+1/2}^{n} + \frac{1}{2a} \overrightarrow{W}_{0,j}^{n+1-} \{gh\partial_x z\}_{j-1/2}^{n}.$$

Finally, since

$$(\Pi u)_{0,j}^{n+1-} = \frac{(\overrightarrow{W}_{0,j}^{n+1-})^2 - (\overleftarrow{W}_{0,j}^{n+1-})^2}{4a}, \quad (\Pi u)_{p,j}^{n+1-} = \frac{(\overrightarrow{W}_{p,j}^{n+1-})^2 - (\overleftarrow{W}_{p,j}^{n+1-})^2}{4a},$$

and

$$\frac{(\overrightarrow{W}_{p,j}^{n+1-})^2 - (\overleftarrow{W}_{0,j+1}^{n+1-})^2}{4a} = \pi_{j+1/2}^{*,n+1-} u_{j+1/2}^{*,n+1-},$$

one easily gets

$$\begin{aligned}
&\overline{(hE)}_j^{n+1-} - \overline{(hE)}_j^{n} + \frac{\Delta t}{\Delta x} \left[\pi_{j+1/2}^{*,n+1-} u_{j+1/2}^{*,n+1-} - \pi_{j-1/2}^{*,n+1-} u_{j-1/2}^{*,n+1-} \right] \\
&\qquad + \sum_{i=0}^{p} \frac{\omega_i}{2} \left(L_{i,j}^{n+1-} - 1\right)(hE)_{i,j}^{n+1-} \leq -\Delta t \, \{ghu\partial_x z\}_j^{n+1-}. \quad (32)
\end{aligned}$$

The transport step. It has already been shown that under the CFL condition (27), $\overline{X}_j^{n+1}$ is a convex combination of $X_{i,j}^{n+1-}$, $X_{p,j-1}^{n+1-}$ and $X_{0,j+1}^{n+1-}$ for $X = h, hu$. Since the function $(h, hu) \mapsto (hE)(h, hu)$ is a convex function, the Jensen inequality implies

$$\begin{aligned}
(hE)(\overline{\boldsymbol{U}}_j^{n+1}) \leq \sum_{i=0}^{p} &\left(\frac{w_i}{2} - \frac{\Delta t}{\Delta x} \left[\int_{\kappa_j} u^{\alpha} \partial_x \phi_{i,j} - \delta_{i,p} \left(u_{j+1/2}^{*,\alpha} \right)_- + \delta_{i,0} \left(u_{j-1/2}^{*,\alpha} \right)_+ \right] \right) (hE)_{i,j}^{n+1-} \\
&- \delta_{i,p} \frac{\Delta t}{\Delta x} \left(u_{j+1/2}^{*,\alpha} \right)_- (hE)_{0,j+1}^{n+1-} + \delta_{i,0} \frac{\Delta t}{\Delta x} \left(u_{j-1/2}^{*,\alpha} \right)_+ (hE)_{p,j-1}^{n+1-}.
\end{aligned}$$

We can rewrite this inequality as follows,

$$\begin{aligned}
&(hE)(\overline{\boldsymbol{U}}_j^{n+1}) - \overline{(hE)}_j^{n+1-} + \frac{\Delta t}{\Delta x} \left[(hE)_{j+1/2}^{*,n+1-} u_{j+1/2}^{*,n+1-} - (hE)_{j-1/2}^{*,n+1-} u_{j-1/2}^{*,n+1-} \right] \\
&\qquad \leq \sum_{i=0}^{p} \frac{\omega_i}{2} \left(L_{i,j}^{n+1-} - 1\right)(hE)_{i,j}^{n+1-}, \quad (33)
\end{aligned}$$

where we have set

$$(hE)^{n+1-}_{j+1/2} = \begin{cases} (hE)^{n+1-}_{p,j} & \text{if} \quad u^*_{j+1/2} \geq 0, \\ (hE)^{n+1-}_{0,j+1} & \text{otherwise.} \end{cases}$$

Finally, combining (32) and (33) we obtain the expected entropy inequality

$$\begin{aligned} &(hE)(\overline{\boldsymbol{U}}^{n+1}_j) - \overline{(hE)}^n_j \\ &\qquad + \frac{\Delta t}{\Delta x}\left[\left(\pi^{*,n+1-}_{j+1/2} + (hE)^{*,n+1-}_{j+1/2}\right) u^{*,n+1-}_{j+1/2} - \left(\pi^{*,n+1-}_{j-1/2} + (hE)^{*,n+1-}_{j-1/2}\right) u^{*,n+1-}_{j-1/2}\right] \\ &\qquad\qquad \leq -\Delta t \, \{ghu\partial_x z\}^{n+1-}_j . \end{aligned}$$